engineering proceedings

MDPI

Proceeding Paper

Production Parameters and Thermo-Mechanical Performance of Twisted and Coiled Artificial Muscles (TCAMs) †

Salvatore Garofalo *, Chiara Morano, Leonardo Pagnotta and Luigi Bruno

Department of Mechanical, Energy and Management Engineering, University of Calabria, Via P. Bucci 44C, 87036 Rende, Italy; chiara.morano@unical.it (C.M.); leonardo.pagnotta@unical.it (L.P.); luigi.bruno@unical.it (L.B.)

* Correspondence: salvatore.garofalo@unical.it

† Presented at the 53rd Conference of the Italian Scientific Society of Mechanical Engineering Design (AIAS 2024), Naples, Italy, 4–7 September 2024.

Abstract: High-strength polymer fibers such as nylon 6, nylon 6,6, and polyethylene are utilized to produce Twisted and Coiled Artificial Muscles (TCAMs) through the twisting of low-cost fibers. These artificial muscles exhibit high displacement and specific power, particularly under electrothermal actuation, which requires conductive elements. An experimental setup was developed to produce, thermally treat, and characterize commercially available nylon 6,6 fibers coated with silver. The results demonstrate that TCAMs can contract by over 15% and generate forces up to 2.5 N with minimal energy input. Key factors such as motor speed, applied load, and fiber geometry affect the overall performance.

Keywords: artificial muscle; twisted and coiled polymer; actuator; smart material

check for updates

Academic Editors: Umberto Galietti, Gabriele Arcidiacono, Enrico Armentani, Davide Castagnetti, Vigilio Fontanari, Aurelio Somà and Nicola Bonora

Published: 13 February 2025

Citation: Garofalo, S.; Morano, C.; Pagnotta, L.; Bruno, L. Production Parameters and Thermo-Mechanical Performance of Twisted and Coiled Artificial Muscles (TCAMs). *Eng. Proc.* **2025**, *85*, 1. https://doi.org/10.3390/engproc2025085001

Copyright: © 2025 by the authors. Licensee MDPI, Basel, Switzerland. This article is an open access article distributed under the terms and conditions of the Creative Commons Attribution (CC BY) license (https://creativecommons.org/licenses/by/4.0/).

1. Introduction

In 2014, Haines and his research group [1] demonstrated how certain polymeric fibers, often made of nylon or polyethylene, could be transformed into artificial muscles with remarkable actuation capabilities. These polymeric materials serve as a fundamental starting point for creating highly efficient artificial muscles due to their unique combination of properties, including excellent reversible thermal contraction along the fiber axis, significant volumetric thermal expansion, and strong anisotropy in heat-induced dimensional changes. Nylon and polyethylene are composed of flexible polymer chains highly oriented along the fiber direction. Such polymer materials consist of crystalline regions with very low negative thermal expansion coefficients and adjacent amorphous regions where polymer chains are intrinsically much freer to move, thus enabling greater contraction. For instance, nylon 6,6 fibers, when heated, can exhibit contractions of around 4%, which is comparable to common Shape Memory Alloy (SMA) filaments (NiTi). These contractions can be further maximized by inducing a radical change in the geometry of the precursor fiber, which must be twisted onto itself to form a helical structure [2].

In recent years, research in the field of artificial muscles and smart materials has grown impressively to meet increasingly stringent demands in many application contexts, from wearable robotics to actuator miniaturization. However, as highlighted by a recent review on the transition from conventional actuators to artificial muscles [3], most smart materials found in the literature still face significant disadvantages. SMAs, for example, while characterized by excellent force capabilities, are particularly expensive and suffer from limited displacement capacities as well as issues related to their inherently hysteretic behavior. Similarly, Electroactive Polymers (EAPs), especially Dielectric Elastomers (DEs), are characterized by excellent actuation speeds and low energy consumption but have extremely

limited force and displacement capabilities. Even Pneumatic Artificial Muscles (PAMs), such as McKibben muscles, are known for their significant displacement capabilities and output power, but they are particularly cumbersome to integrate, especially in wearable devices due to the need for compressors. Twisted and Coiled Artificial Muscles (TCAMs) thus offer an excellent alternative to all the actuation technologies mentioned above, although they still present some disadvantages, such as limited bandwidth and particularly high energy consumption. These artificial muscles are also extremely cost-effective as they are made from polymer fibers such as fishing or sewing thread. For this reason, TCAMs are often referred to as Twisted and Coiled Polymers (TCPs). They are frequently produced from composite precursor fibers containing conductive elements like carbon nanofibers [4] or featuring thin layers of silver, copper, or other conductive elements on the outside. This is because, while TCAMs can be actuated in various ways, such as hydrothermal, chemical, or photonic energy, the simplest and most effective method is electrothermal actuation via the Joule effect [5]. The presence of conductive elements becomes essential due to the intrinsically non-conductive nature of polymeric materials. Therefore, referring to TCAMs as Twisted and Coiled Composites (TCCs) would be more accurate.

Figure 1 illustrates the step-by-step process for properly creating a TCAM [6]. As can be seen, the first phase of the production process is the twisting phase: a precursor fiber is attached at one end to an electric motor that rotates it at a specific speed, while weight is attached to the other end to keep the filament under tension throughout the process. It is important to note that the attached weight plays a fundamental role. A weight that is too heavy risks breaking the filament before the twisting phase is completed, while a weight that is too light would result in entanglement. Additionally, as will be discussed in the Results and Discussion Section, the motor's rotational speed is another critical parameter in determining the performance of the resulting artificial muscle. Even the direction of motor rotation, and particularly the directions of twisting and coiling, play an important role in establishing the performance of TCAMs. When the directions of twisting and coiling coincide, the resulting muscle is said to be homochiral and exhibits a negative thermal expansion coefficient (it contracts when actuated); conversely, if the twisting and coiling directions differ, the artificial muscle is said to be heterochiral and exhibits a positive thermal expansion coefficient (it expands when actuated). These thermal properties are completely independent of the intrinsic properties of the precursor material, as they are purely associated with the geometric characteristics of the actuator [7].

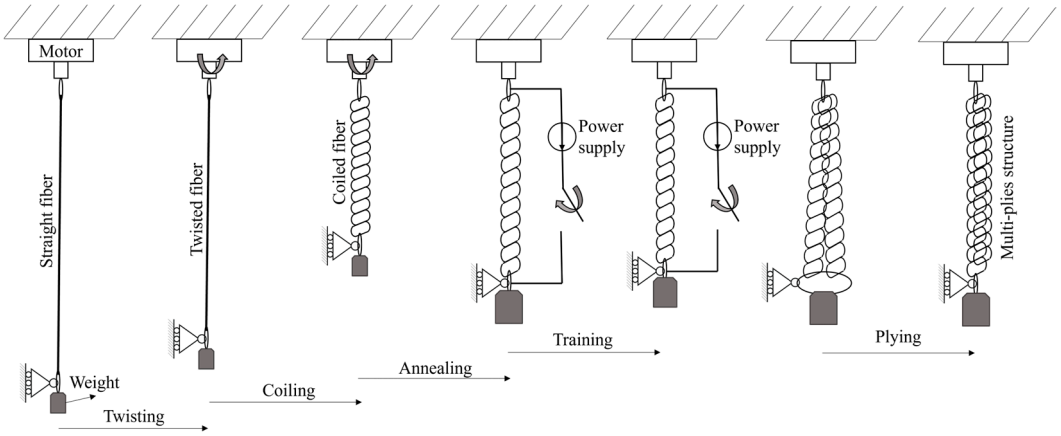


Figure 1. Manufacturing process of TCAM: twisting and coiling are necessary to create the structure of the artificial muscle; annealing and training allow to relax stress during the previous steps and set the geometry; plying is needed when multi-plies geometries are required.

During the twisting phase, the precursor fiber can absorb a certain amount of torsion within itself. Indeed, when the torque reaches a critical value, as defined by Equation (1) [8,9], the fiber begins to twist upon itself, forming a geometric structure resembling a spring (coiled fiber).

$$\tau_c = \sqrt{2EIF}. \tag{1}$$

In Equation (1), E represents the Young's modulus of the material, I is the moment of inertia of a fiber with a circular cross-section and diameter D, as given by Equation (2), while F is the force generated by the weight applied to the fiber, which produces a stress σ provided by Equation (3).

$$I = \frac{\pi}{64} D^4, \tag{2}$$

$$\sigma = \frac{4F}{\pi D^2}. \tag{3}$$

At this point, as also reported by Haines et al. [9], the critical torsion value, expressed in twists per meter, which causes the fiber to twist upon itself, is given by Equation (4):

$$T_c = \frac{\tau_c}{2\pi JG}, \tag{4}$$

$$J = \frac{\pi}{32} D^4, \tag{5}$$

where J represents the polar moment of inertia of the fiber's circular cross-section, as provided by Equation (5), and G is its shear modulus. Consequently, by combining Equations (1) and (4), the expression for the critical torsion (Equation (6)) necessary to twist the fiber upon itself under the action of stress σ is obtained.

$$T_c = \frac{\sqrt{2\sigma E}}{\pi DG}. \tag{6}$$

Once the twisting and coiling phases are complete, the artificial muscle remains highly unstable. The previous production stages have generated residual stresses within its structure, which must be relaxed. To achieve this, as shown in Figure 1, an appropriate heat treatment is required. It is important to note that this process can be carried out in an oven if the precursor fiber is purely polymeric; however, if the fiber is composite and contains any conductive element on or within it, the heat treatment can be performed electrothermally, utilizing Joule heating. Typically, when electrothermal treatment is applied, 12 On/Off cycles are carried out, with each cycle lasting 60 s (duty cycle = 50%), while passing a current through the artificial muscle ranging from 0.1 to 0.7 A, depending on the initial dimensions of the fiber. As shown in Figure 1, when transitioning from the coiling to the annealing phase, the weight applied to the fiber's end must be slightly increased to allow adjacent coils to disentangle, thus maximizing the displacement capacity of the resulting actuator.

The next phase is the training phase. This phase is designed to "train" the artificial muscle to perform its specific task. The weight applied to the fiber during the training phase must be reduced again to match the weight the muscle is expected to handle in actual operation. This phase can also be conducted using electrothermal actuation if the precursor fiber is a composite containing conductive elements within it. Once the twisting, coiling, annealing, and training phases are completed, a final phase, known as plying, could be performed. In this phase, two or more muscles with identical geometric and electrical characteristics are twisted together to form a sort of artificial muscle bundle. This process would, of course, enhance the actuator's force capacity, albeit at the expense of its displacement capability.

Despite the numerous advantages described so far, TCAMs are still rarely applied, and when they are, it is mostly in robotic contexts. The reason is likely twofold. In fact, this type of artificial muscle, as initially introduced, is relatively new, having been developed only about a decade ago. Additionally, there are still few studies on their thermo-electro-mechanical performance, as well as analyses of their fatigue life and the most appropriate control technologies.

In light of the analysis conducted so far, the following work aims to examine the thermo-mechanical behavior of TCAMs. To achieve this, an experimental setup was developed for the three different phases of the analysis: production, heat treatment, and characterization. The precursor fibers used are commercially available and composed of nylon 6,6 with a thin layer of silver applied externally to ensure electrothermal actuation. These fibers were tested using various production parameters and characterized in terms of force capacity and displacement. The results highlight that TCAMs are capable of sustaining contractions exceeding 15% and delivering controlled forces of up to 2.5 N, with very low input currents and voltages. The experimental investigation also allowed for the observation of how motor rotational speed, applied weight, electrical power, and the geometric shape of the precursor fiber influence the mechanical performance of these artificial muscles.

2. Materials and Methods

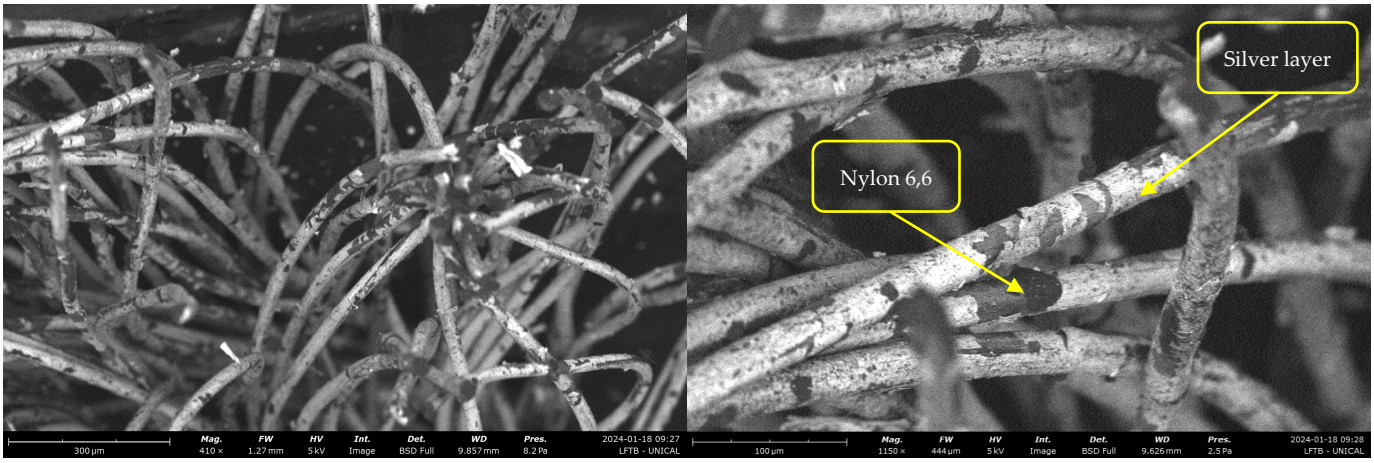
2.1. Experimental Section

2.1.1. Materials

As anticipated in the previous section, the experimentation involved the analysis of the thermo-mechanical performance of three different types of precursor fibers used to create TCAMs. Specifically, the precursor fibers in question are Shieldex 117/17x2 HCB, Shieldex 235/36x2 HCB, and Shieldex 235/36x4 HCB, which are multi-filament structures composed of nylon 6,6 externally coated with a thin layer of silver. The aforementioned nomenclature provides important information regarding the geometry of the precursor filaments. Specifically:

- The first number indicates the linear density of the fibers expressed in dtex, a typical unit of measurement for filaments that stands for grams per 10 km;
- The second value indicates the number of filaments present in a single layer of the precursor fiber;
- The third value, finally, indicates the total number of layers present.

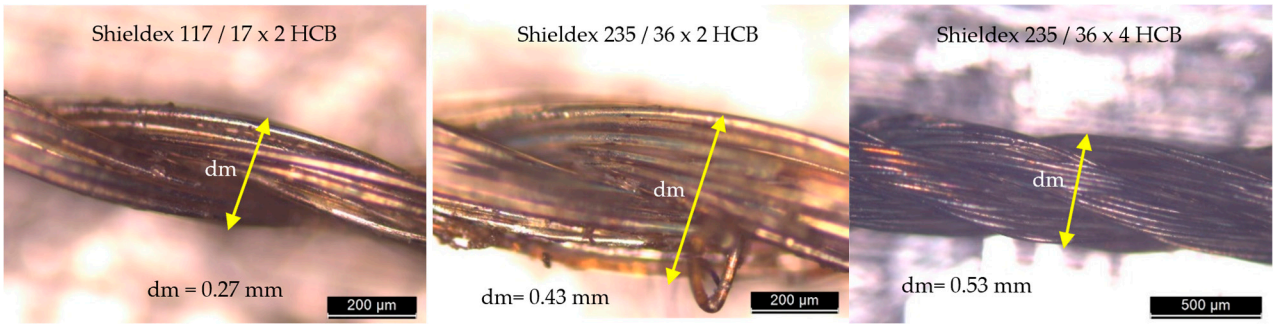
From the provided details, it is clear that the precursor fibers used are extremely thin strands obtained by twisting individual filaments together. To better understand the structure of the precursor fibers used in the experimental analysis, SEM (Scanning Electron Microscope) analyses were conducted. Figure 2 presents two images obtained from SEM investigations referring to the Shieldex 235/36x4 fibers, but the same identical structures can be found in the other two types of precursor fibers. As can be seen, the individual filaments that make up the strands have an average diameter of about 25 μm. Additionally, the SEM images clearly distinguish the two materials that constitute the filaments: it is evident that their core is made of nylon 6,6, while externally, there is a thin layer of silver randomly applied to the nylon surface, leaving small portions of the nylon underneath exposed. On the outer surface, as indicated by the data sheets of the fibers analyzed, there is nitrile rubber, necessary to counteract the action of atmospheric agents.



(**a**) (**b**)

Figure 2. SEM analysis performed on the precursor fibers: (**a**) SEM image obtained of the Shieldex 235/36x4 HCB precursor fiber; (**b**) SEM magnification of (**a**).

Figure 3 presents the micrographs taken of the precursor fibers. As can be observed, and as was evident from the previously mentioned fiber nomenclature, the thinnest fiber is the Shieldex 117/17x2 HCB, with an average diameter of 270 µm. Following this is the Shieldex 235/36x2 HCB, which has an average diameter of 430 µm, and finally, the Shieldex 235/36x4 HCB, with a diameter of approximately 530 µm. The images in Figure 3 also show the overall structure of the precursor fibers. Notably, the first two fibers (Figure 3a,b) consist of only two layers, while the third fiber (Figure 3c) is characterized by the presence of four distinct layers wrapped together.



(**a**) (**b**) (**c**)

Figure 3. Micrographs taken of the precursor fibers and determination of their average diameters: (**a**) Shieldex 117/17x2 HCB; (**b**) Shieldex 235/36x2 HCB; (**c**) Shieldex 235/36x4 HCB.

2.1.2. Experimental Setup

Figure 4 shows the experimental setup used for the tests. On the right, there is a schematic of the setup, while on the left, its realization is shown. The setup consists of the following:

- A laser displacement sensor (Micro-Epsilon optoNCDT 1220-500 mm, Ortenburg, Germany) for displacement detection;
- A 12 V DC motor with a planetary gear and digital encoder used during the twisting and coiling phases of the artificial muscles;
- A 3D-printed weight holder with an aluminum rod at its base for attaching weights during the different phases of production and characterization;

- A guide for the weight holder, also made via 3D printing, necessary to direct the movement of the holder and avoid undesired movements;
- A control unit;
- An Arduino UNO Rev3 board used to control the speed and rotation direction of the DC motor via the digital encoder mounted on it;
- A power supply (Aim TTi CPX series 400DP) used to power the electric motor and actuate the artificial muscles.

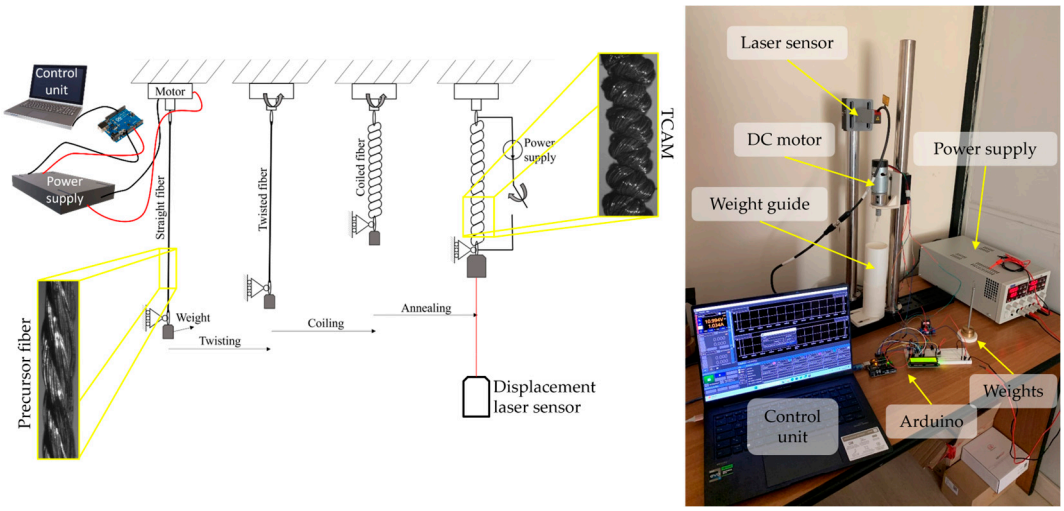


Figure 4. Schematic representation of the experimental setup (on the **left**) and its prototyping (on the **right**).

3. Results and Discussion

3.1. Results for Constant Actuation Currents

Moving on to the analysis of the results, it is important to note that different tests were conducted by varying a series of parameters considered fundamental in determining the performance of TCAMs. Specifically, compared to what is found in the literature [6,7], the main parameters that significantly influence the performance of these artificial muscles are the rotational speed ω of the electric motor during the twisting and coiling phases, the production weight P_p, the annealing weight P_a, and the magnitude I of the actuation current. Since this work focused exclusively on characterizing TCAMs as a function of production parameters, the training phase was bypassed as it was considered unnecessary. In essence, after producing the artificial muscles and performing thermal treatment for stabilization, they were directly subjected to the working phase.

Table 1 lists the loads used during the production (twisting and coiling), thermal treatment, and working phases of the muscles made from Shieldex 235/36x4 HCB fibers. The logic followed is described below and applies to muscles made from the other two types of precursor fibers as well (Tables 2 and 3). For each test, a specific load was set during the production phase, which was then increased during the thermal treatment phase to allow adjacent coils to disentangle and increase the muscle's contraction capacity. Finally, during the working phase, the load was set equal to that used during the previous thermal treatment phase. Of course, the loads in the three diverse tables differ because, as seen earlier, the initial dimensions of the precursor fibers change.

Table 1. Loads used with the Shieldex 235/36x4 HCB fiber during the different phases.

Production	Annealing	Working
P = 0.79 N	P = 1.28 N	P = 1.28 N
P = 1.18 N	P = 1.67 N	P = 1.67 N
P = 1.57 N	P = 2.06 N	P = 2.06 N
P = 1.77 N	P = 2.26 N	P = 2.26 N

Table 2. Loads used with the Shieldex 235/36x2 HCB fiber during the different phases.

Production	Annealing	Working
P = 0.40 N	P = 0.69 N	P = 0.69 N
P = 0.49 N	P = 0.79 N	P = 0.79 N
P = 0.59 N	P = 0.89 N	P = 0.89 N
P = 0.69 N	P = 1 N	P = 1 N

Table 3. Loads used with the Shieldex 117/17x2 HCB fiber during the different phases.

Production	Annealing	Working
P = 0.29 N	P = 0.49 N	P = 0.49 N
P = 0.39 N	P = 0.59 N	P = 0.59 N
P = 0.49 N	P = 0.69 N	P = 0.69 N
P = 0.59 N	P = 0.79 N	P = 0.79 N
P = 0.69 N	P = 0.89 N	P = 0.89 N
P = 0.79 N	P = 1 N	P = 1 N

Regarding the results, Figures 5–7 display the outcomes obtained for TCAMs produced from the Shieldex 235/36x4 HCB, Shieldex 235/36x2 HCB, and Shieldex 117/17x2 HCB fibers, respectively. Each figure presents a graph containing a series of curves in different colors. Specifically, distinct colors correspond to different rotational speeds of the electric motor during the production phase: red curves (ω = 300 rpm), blue curves (ω = 600 rpm), and black curves (ω = 900 rpm).

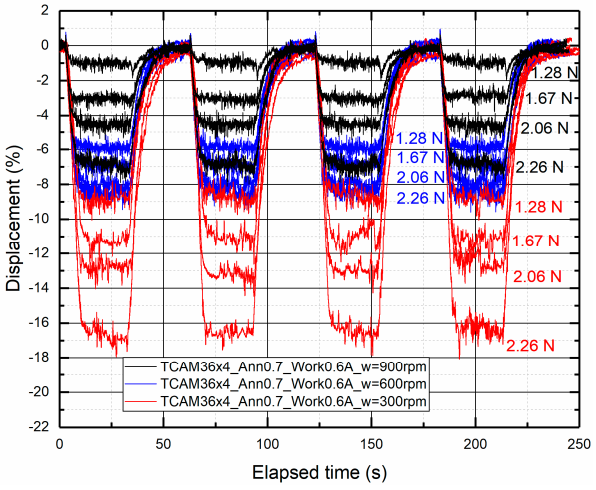


Figure 5. Results of percentage displacement obtained for TCAMs made from the Shieldex 235/36x4 HCB fiber at the three rotational speeds during production: ω = 300 rpm (red curve); ω = 600 rpm (blue curve); ω = 900 rpm (black curve). The tests were conducted with a supply current of 0.6 A.

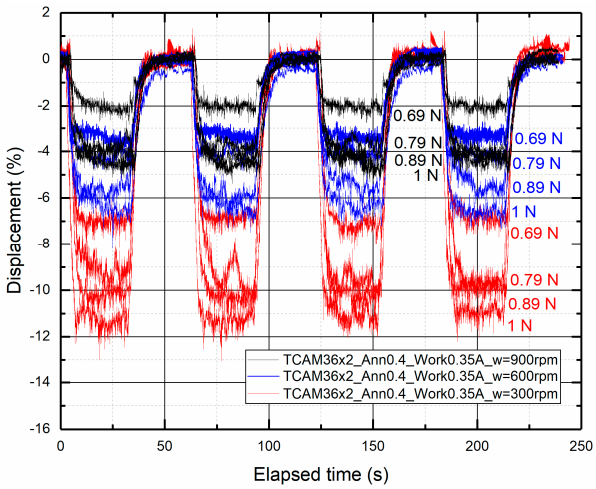


Figure 6. Results of percentage displacement obtained for TCAMs made from the Shieldex 235/36x2 HCB fiber at the three rotational speeds during production: ω = 300 rpm (red curve); ω = 600 rpm (blue curve); ω = 900 rpm (black curve). The tests were conducted with a supply current of 0.35 A.

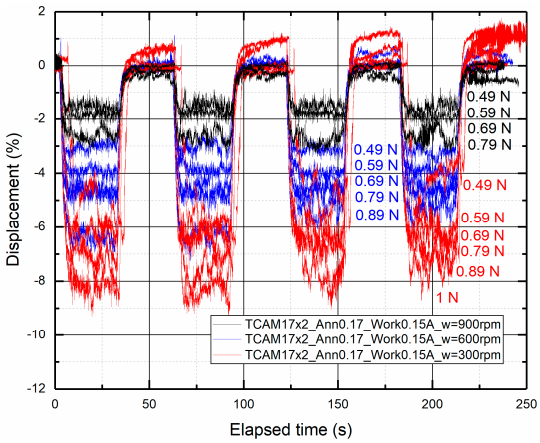


Figure 7. Results of percentage displacement obtained for TCAMs made from the Shieldex 117/17x2 HCB fiber at the three rotational speeds during production: ω = 300 rpm (red curve); ω = 600 rpm (blue curve); ω = 900 rpm (black curve). The tests were conducted with a supply current of 0.15 A.

During the production process, achieving muscles of identical length is a complex task, leading to slight variations in their dimensions. Therefore, to compare the contraction capacity of TCAMs produced under different parameters, the displacement of each muscle was normalized by dividing it by its initial length. This normalization explains why, in each graph, the displacement is expressed as a percentage.

The tests were conducted under current-controlled conditions, with voltage adjustments made to account for variations in the muscles' resistance. Each plateau in the graphs corresponds to the maximum contraction of the muscles, achieved under the respective load and power input.

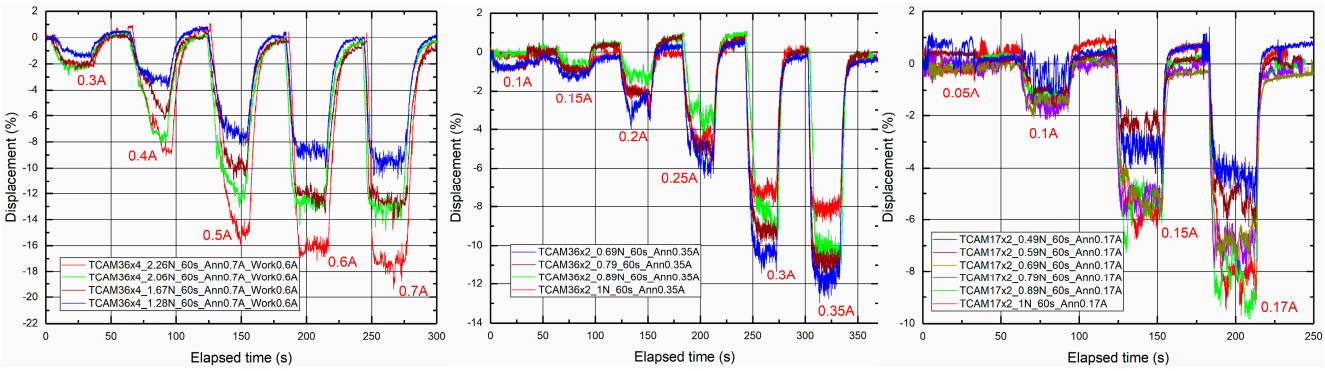
By carefully examining each figure, two significant experimental results can be extrapolated, which are consistent with the findings reported in the literature [7]. Firstly, it is observed that, at the same DC motor rotational speed during production, a higher applied load on the artificial muscle results in a higher contraction capacity. This result aligns with the load condition: a higher load induces a greater pre-strain in the muscle, leading to a significantly enhanced contraction. Specifically, as the applied load increases, the disentanglement between coils becomes more pronounced, thereby enhancing the muscle's contraction capability. Additionally, it is also noted that, for the same load, increasing

the DC motor rotational speed during production reduces the contraction capacity of the artificial muscles. This result is related to the fact that as the rotational speed increases, the production of TCAMs becomes increasingly uncontrolled. Consequently, the coils constituting the artificial muscle exhibit more imperfections, which adversely affects their mechanical performance in terms of displacement capacity.

Furthermore, it is important to note that results for Shieldex 117/17x2 HCB (Figure 7) highlight an additional consideration. Indeed, as the DC motor rotational speed increases, the muscle structure becomes increasingly unstable, making certain results not achievable. Specifically, shifting from ω = 300 rpm to ω = 600 rpm prevents the fabrication of muscle loaded with 1 N; similarly, transitioning from ω = 600 rpm to ω = 900 rpm does not permit the production of muscle with 0.89 N. This instability explains why some curves are absent at higher DC motor rotational speeds in Figure 7.

3.2. Results for Increasing Actuation Currents

While the previous section analyzed the experimental results obtained by powering the artificial muscles with a constant current, this section presents and examines the results obtained by powering the TCAMs with increasing supply currents. Figure 8 shows the results in terms of contraction capacity for the muscles made from all three types of precursor fibers analyzed, achieved with a DC motor rotational speed of ω = 300 rpm during production. Only the results for ω = 300 rpm are reported here because, as observed in the previous section, lower production speeds yield better contraction performance. However, it is important to note that the same considerations apply to the other two tested speeds, ω = 600 rpm and ω = 900 rpm.



(**a**) (**b**) (**c**)

Figure 8. Experimental results in terms of displacement obtained for TCAMs produced with a DC motor rotational speed of ω = 300 rpm, using increasing supply currents. The graphs refer to the following precursor fibers: (**a**) Shieldex 235/36x4 HCB; (**b**) Shieldex 235/36x2 HCB; (**c**) Shieldex 117/17x2 HCB.

Examining the graphs in Figure 8, it is first observed that as the supply current increases, the displacement capacity of the artificial actuator also increases, regardless of the applied load. This indicates that TCAMs are extremely sensitive to the magnitude of the supply current. Furthermore, as seen in the graphs, the slopes of each new segment of actuation tend to become steeper as the supply current increases. In other words, the higher the current applied to the actuator, the faster it tends to contract. This phenomenon is primarily related to an electrothermal concept. As the supply current increases, the rate at which the muscle heats up also increases, and consequently, the rate at which it reaches its maximum contraction speeds up.

4. Conclusions

In this work, significant experimental results were obtained regarding the production and characterization of TCAMs. The main result shows that TCAMs made from nylon 6,6 fibers coated with silver exhibit a contraction capacity greater than 15%, with forces delivered close to 2.5 N and with low energy input. Additionally, a notable effect of production parameters on the performance of these artificial muscles was observed. Specifically, it was found that motor rotational speed and the load applied during the twisting and coiling phases significantly influence the contraction capacity. Furthermore, TCAMs exhibit considerable sensitivity to the actuation current. In fact, as the actuation current increases, the contraction capacity of the TCAMs increases, resulting in a faster response to electrothermal stimuli. Despite these remarkable results, TCAMs are still rarely applied in practice due to their relatively recent development and the need for further experimental investigations to fully characterize them. For example, a systematic evaluation of the long-term durability of TCAMs is still lacking. It would therefore be useful to investigate the long-term behavior of these muscles under repeated actuation cycles. Moreover, it was observed that the cooling rate influences the muscle's response, and preliminary results suggest that forced cooling could improve dynamic performance. Further studies could thus explore different cooling methods with the aim of optimizing response times.

Author Contributions: Conceptualization, S.G. and L.B.; methodology, S.G. and L.B.; formal analysis, S.G. and L.B.; investigation, S.G.; resources, S.G. and L.B; writing—original draft preparation, S.G.; writing—review and editing, S.G. and C.M.; visualization, L.B.; supervision, L.B. and L.P.; project administration, L.B. All authors have read and agreed to the published version of the manuscript.

Funding: This research received no external funding.

Institutional Review Board Statement: Not applicable.

Informed Consent Statement: Not applicable.

Data Availability Statement: Data are contained within the article.

Acknowledgments: We acknowledge co-funding from Next Generation EU, in the context of the National Recovery and Resilience Plan, Investment PE8—Project Age-It: "Ageing Well in an Ageing Society", CUP H23C22000870006. This resource was co-financed by the Next Generation EU [DM 1557 11.10.2022]. The views and opinions expressed are only those of the authors and do not necessarily reflect those of the European Union or the European Commission. Neither the European Union nor the European Commission can be held responsible for them.

Conflicts of Interest: The authors declare no conflict of interest.

References

1. Haines, C.S.; Lima, M.D.; Li, N.; Spinks, G.M.; Foroughi, J.; Madden, J.D.W.; Kim, S.H.; Fang, S.; Jung De Andrade, M.; Göktepe, F.; et al. Artificial Muscles from Fishing Line and Sewing Thread. *Science* **2014**, *343*, 868–872. [CrossRef] [PubMed]
2. Yuan, J.; Poulin, P. Fibers Do the Twist. *Science* **2014**, *343*, 845–846. [CrossRef] [PubMed]
3. Garofalo, S.; Morano, C.; Perrelli, M.; Pagnotta, L.; Carbone, G.; Mundo, D.; Bruno, L. A Critical Review of Transitioning from Conventional Actuators to Artificial Muscles in Upper-Limb Rehabilitation Devices. *J. Intell. Mater. Syst. Struct.* **2024**, *35*, 1263–1290. [CrossRef]
4. Lamuta, C.; Messelot, S.; Tawfick, S. Theory of the Tensile Actuation of Fiber Reinforced Coiled Muscles. *Smart Mater. Struct.* **2018**, *27*, 055018. [CrossRef]
5. Suzuki, M.; Kamamichi, N. Control of Twisted and Coiled Polymer Actuator with Anti-Windup Compensator. *Smart Mater. Struct.* **2018**, *27*, 075014. [CrossRef]
6. Saharan, L.; Tadesse, Y. Novel Twisted and Coiled Polymer Artificial Muscles for Biomedical and Robotics Applications. In *Materials for Biomedical Engineering*; Elsevier: Amsterdam, The Netherlands, 2019; pp. 45–75. ISBN 978-0-12-816909-4.

7. Saharan, L.; Tadesse, Y. Fabrication Parameters and Performance Relationship of Twisted and Coiled Polymer Muscles. In *Volume 14: Emerging Technologies; Materials: Genetics to Structures; Safety Engineering and Risk Analysis, Proceedings of the ASME 2016 International Mechanical Engineering Congress and Exposition, Phoenix, AZ, USA, 11–17 November 2016*; American Society of Mechanical Engineers: Phoenix, AZ, USA; p. V014T11A028.
8. Ross, A.L. Cable Kinking Analysis and Prevention. *J. Eng. Ind.* **1977**, *99*, 112–115. [CrossRef]
9. Haines, C.S.; Li, N.; Spinks, G.M.; Aliev, A.E.; Di, J.; Baughman, R.H. New Twist on Artificial Muscles. *Proc. Natl. Acad. Sci. USA* **2016**, *113*, 11709–11716. [CrossRef] [PubMed]

Disclaimer/Publisher's Note: The statements, opinions and data contained in all publications are solely those of the individual author(s) and contributor(s) and not of MDPI and/or the editor(s). MDPI and/or the editor(s) disclaim responsibility for any injury to people or property resulting from any ideas, methods, instructions or products referred to in the content.